Machine Vibration (1996) 5:131–141

Machine Vibration

The Nonlinear Response and Passive Vibration Isolation of Rigid Bodies

R. Matthew Brach[1] and Alan G. Haddow[2]

[1]Advanced Vehicle Technology, Ford Motor Company, Dearborn, USA, [2]Department of Mechanical Engineering, Michigan State University, East Lansing, USA

The nonlinear response of an automotive engine on mounts is investigated. The engine and mount system is represented by a planar three degree of freedom system consisting of a rigid body connected to ground through flexible supports. The nonlinear response of this three degree of freedom system is established using the method of multiple scales. A representative frequency response of the system is presented using parameter values associated with an in-line four cylinder engine running at hot idle. This frequency response shows that when 1:1 and 2:1 internal resonances exist between the linear natural frequencies of the system, multiple steady state solutions can exist. This nonlinear system response occurs due to the system geometry and therefore nonlinear force–deflection characteristics of the flexible supports are not required. Additionally, the isolation characteristics of the system are established based on the system response. The efficient transfer of energy from one mode to another is exploited to enhance the isolation performance of the system.

Keywords: Engine; Isolation; Mount; Nonlinear; Vibration

1. Introduction

This paper presents the results of an analytical investigation into the harmonic response and vibration isolation characteristics of a three degree of freedom rigid body system. There are two main components to the work. The first deals with the complex type of responses that can occur in what might seem to be a relatively simple rigid body system. The second deals with the issue of defining a meaningful measure of the performance of an isolator when multiple degrees of freedom are present. Since the motivation for the work was to better understand the planar dynamic behaviour of an automotive engine on flexible mounts, reference is made throughout to such a physical system. Moreover, parameter values in keeping with an in-line four cylinder engine are used in the numerical examples that are given.

The system is modelled with supports possessing linear force displacement characteristics, and the equations of motion for the system are derived allowing for general motion of the rigid body, i.e., no small motion assumption is made. This leads to nonlinear equations of motion. An approximate solution to these equations of motion is found using the method of multiple scales, see, for example, Nayfeh and Mook [1]. A representative frequency response of the system for parameter values associated with an in-line four cylinder engine, shows that when 1:1 and 2:1 internal resonances exist between the linear natural frequencies of the system, multiple steady state solutions can exist. In addition, the nonlinear response may be accompanied by a transfer of energy between modes that can be utilized to improve the isolation performance of the rigid body system. It should be stressed that such a transfer of energy does not necessitate the presence of large motions. It is the existence of the internal tuning condition that causes an exceptionally strong coupling between the modes.

Past studies in this area include the work of Henry and Tobias [2,3]. They examined the unforced nonlinear response of a two degree of freedom, rigid body, isolation system. In particular, the stability of modes and modal coupling of this system were investigated. Grootenhuis and Ewins [4] investigated the unforced response of a six degree of freedom rigid body system on resilient supports. Specifically, the change in the linear natural frequencies of the system as a function of the location of the centre of gravity was examined. Efstathiades and Williams [5] studied the coupled response of two of the six degrees of freedom of a rigid body system with supports at four

Correspondence and offprint requests to: R. M. Brach, Advanced Vehicle Technology, Ford Motor Company, Building 3, MD3047, 20000 Rotunda Drive, Dearborn, MI 48121–2053, USA.

corners. These corner supports were modelled using symmetric cubic force–displacement characteristics. Internal resonances of the system were investigated using the method of harmonic balance. The study showed that through the presence of the nonlinear characteristics of the corner supports and internal resonances, otherwise normal modes of vibration could become coupled.

It is hoped that the results of this study will extend the tools commonly used by automotive engineers to establish engine mount placement, viz., torque axis theory, natural frequency placement, and elastic axis theory. A comprehensive review of these three analysis techniques is given in Brach [6].

2. Physical System

2.1 System Description

The system analysed in this paper is based on the geometry of a planar, three degree of freedom rigid body mounted on resilient supports with linear force–deflection characteristics. A schematic of the model is shown in Fig. 1. The damping is assumed to be light and is simply added to each modal coordinate after the equations have been derived. Each of the supports is characterized by two orthogonal stiffness values, one for the lateral stiffness and one for the axial stiffness.

The dimensions, physical parameters, and operating conditions associated with the rigid body utilized in the analysis correspond closely to a four-cylinder automotive engine at hot idle. The support characteristics are representative of actual elastomeric engine mounts. The geometry of the system analysed in this paper is symmetric as shown in Fig. 2. This symmetry is not typical of an actual engine but is introduced to make the problem more tractable and to facilitate the interpretation of the system response.

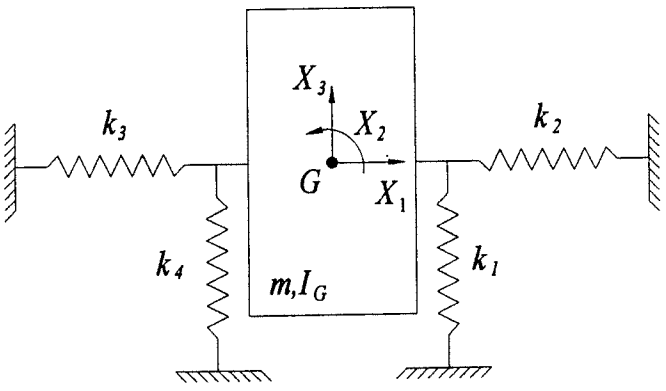

Fig. 1. Geometry of the rigid body system.

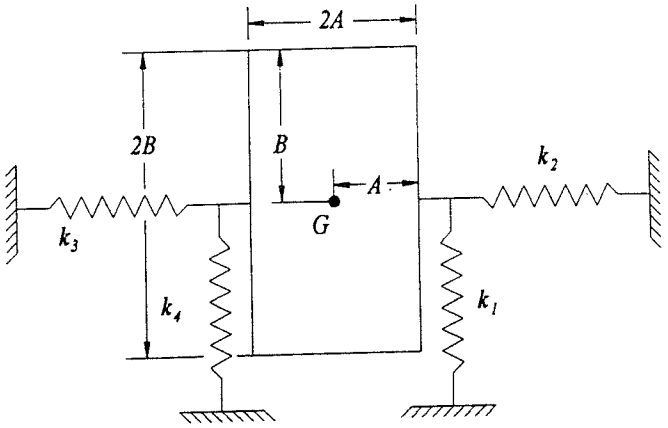

Fig. 2. Physical dimensions of the rigid body.

2.2 Equations of Motion

Lagrange's equations are used to derive the equations of motion for this rigid body system. The expression for the kinetic energy of the system can be written directly. However, due to the complexity of the expression for the deflection of each spring, the expression for the potential energy of the system is complex. The computer program Mathematica by Wolfram [7] is used to obtain a Taylor series expansion that is written about the state equilibrium position of the system. The number of terms required for satisfactory performance of the series has been established by Brach [6]. Use of the series renders the final equations of motion for the system in a form such that the nonlinear terms are expressed in polynomial form. After several simplifications are made to the actual equations of motion of the system, the resulting equations analysed for the system response are:

$$\ddot{X}_1 + 2\epsilon\mu_1\omega_1\dot{X}_1 + \omega_1^2 X_1 + \epsilon\alpha_1 X_2 X_3 + \epsilon\alpha_2 X_1 X_3 + \epsilon\alpha_3 X_2^3 + \epsilon\alpha_4 X_1 X_2^2 + \epsilon\alpha_5 X_1^3 + \epsilon\alpha_6 X_1 X_3^2 = f_1(t) \quad (1)$$

$$\ddot{X}_2 + 2\epsilon\mu_2\omega_2\dot{X}_2 + \omega_2^2 X_2 + \epsilon\alpha_7 X_1 X_3 + \epsilon\alpha_8 X_2^3 + \epsilon\alpha_9 X_1 X_2^2 + \epsilon\alpha_{10} X_1^2 X_2 + \epsilon\alpha_{11} X_2 X_3^2 = f_2(t) \quad (2)$$

$$\ddot{X}_3 + 2\epsilon\mu_3\omega_3\dot{X}_3 + \omega_3^2 X_3 + \epsilon\alpha_{12} X_1^2 + \epsilon\alpha_{13} X_1 X_2 + \epsilon\alpha_{14} X_2^2 X_3 + \epsilon\alpha_{15} X_1^2 X_3 + \epsilon\alpha_{16} X_3^3 = f_3(t) \quad (3)$$

The α_j, the coefficients of the nonlinear terms, are complex functions of the geometry of the system. In Section 4.2 actual numerical values are given for a particular case. Damping associated with each mode has been introduced into the equations and is rep-

resented by the μ_j. The dimensionless parameter ϵ has been introduced to provide appropriate ordering of the damping and nonlinear terms required for the subsequent application of the perturbation solution technique.

3. Approximate Solution Technique

Traditional solution techniques cannot be used to find a closed-form solution to Eqs (1), (2), and (3). Therefore an approximate solution to the equations is sought with the use of the perturbation technique known as the method of multiple time scales as presented by Nayfeh and Mook [1]. The next section presents a brief description of the method and the following sections apply the method to obtain an approximate solution to the equations of motion of this system.

3.1 The Method of Multiple Scales

The fundamental notion of the method of multiple scales is to consider series expansions representing the solution to differential equations, such as Eqs (1), (2), and (3) above, as a function of multiple independent variables, or scales, instead of as a function of a single variable. In the case of the method of multiple scales the variable treated this way is time, t. This transition to multiple independent variables is accomplished by writing time in the following manner:

$$T_n = \epsilon^n t \text{ for } 0 < \epsilon \ll 1 \text{ and } n = 0, 1, 2, \ldots \tag{4}$$

where t is the independent time variable, the T_n are the new independent time variables, and ϵ is an ordering parameter. It transpires that the time T_0 will capture the fast dynamics while ignoring any slowly varying changes. The time T_1 will capture more slowly varying changes, for example a drift in amplitude.

Following the usual procedure of the method of multiple scales and neglecting terms of $O(\epsilon^2)$, the solutions to Eqs (1), (2), and (3) are expressed in the form:

$$X_j(t;\epsilon) = x_{j0}(T_0,T_1) + \epsilon x_{j1}(T_0,T_1) \text{ where } T_0 = t \text{ and } T_1 = \epsilon t \text{ for } j = 1, 2, 3 \tag{5}$$

The derivatives of these expressions with respect to time t become partial derivatives with respect to the different time scales. Accordingly, they become:

$$\frac{d(X_j)}{dt} = (D_0 + \epsilon D_1)(X_j),$$
$$\frac{d^2(X_j)}{dt^2} = (D_0^2 + 2\epsilon D_0 D_1)(X_j) \quad \text{for } j = 1, 2, 3 \tag{6}$$

where

$$D_k(X_j) = \frac{\partial(X_j)}{\partial T_k} \text{ and}$$
$$D_k^2(X_j) = \frac{\partial^2(X_j)}{\partial T_k^2} \text{ for } j = 1, 2, 3, k = 0, 1 \tag{7}$$

The forcing terms in Eqs (1), (2), and (3) can be reordered such that $f_j(t) = \epsilon \hat{f}_j(t)$. Physically this means that the forcing is relatively small, which is valid since it arises from small unbalances in the engine. Utilizing this reordering and substituting the results of Eqs (5), (6), and (7) into Eqs (1), (2), and (3), gives:

$$D_0^2 x_{j0} + \omega_j^2 x_{j0} = 0 \tag{8}$$

$$\begin{aligned} D_0^2 x_{11} + \omega_1^2 x_{11} = &- 2D_0 D_1 x_{10} \\ &- 2\mu_1 \omega_1 D_0 x_{10} \\ &- \alpha_1 x_{20} x_{30} - \alpha_2 x_{10} x_{30} \\ &- \alpha_3 x_{20}^3 \\ &- \alpha_4 x_{10} x_{20}^2 - \alpha_5 x_{10}^3 \\ &- \alpha_6 x_{10} x_{30}^2 + \hat{f}_1 \\ D_0^2 x_{21} + \omega_2^2 x_{21} = &- 2D_0 D_1 x_{20} \\ &- 2\mu_2 \omega_2 D_0 x_{20} \\ &- \alpha_7 x_{10} x_{30} - \alpha_8 x_{20}^3 \\ &- \alpha_9 x_{10} x_{20}^2 \\ &- \alpha_{10} x_{10}^2 x_{20} \\ &- \alpha_{11} x_{20} x_{30}^2 + \hat{f}_2 \\ D_0^2 x_{31} + \omega_3^2 x_{31} = &- 2D_0 D_1 x_{30} - 2\mu_3 \omega_3 D_0 x_{30} \\ &- \alpha_{12} x_{10}^2 + \alpha_{13} x_{10} x_{20} \\ &- \alpha_{14} x_{20}^2 x_{30} - \alpha_{15} x_{10}^2 x_{30} \\ &- \alpha_{16} x_{30}^3 + \hat{f}_3 \end{aligned} \tag{9}$$

The solution to Eqs (8) can be written in the form:

$$x_{j0} = A_j(T_1) e^{(iwjTo)} + cc \quad j = 1, 2, 3 \tag{10}$$

where the use of cc denotes the complex conjugate of the preceding terms. The A_j are complex functions of T_1 and are determined later in the analysis.

Substituting Eqs (10) into Eqs (9), and simplifying leads to:

$$\begin{aligned} D_0^2 x_{11} + \omega_1^2 x_{11} = &- 2A_1' i\omega_1 e^{i\omega_1 T_0} \\ &- 2\mu_1 A_1 i\omega_1^2 e^{i\omega_1 T_0} \\ &- \alpha_1 (A_2 A_3 e^{i(\omega_2 + \omega_1)T_0} + \overline{A}_2 A_3 e^{i(\omega_1 - \omega_2)T_0}) \\ &- \alpha_2 (A_1 A_3 e^{i\omega_1 + \omega_3)T_0} + \overline{A}_1 A_3 e^{i(\omega_3 - \omega_1)T_0}) \\ &- \alpha_3 (A_2^3 e^{3i\omega_2 T_0} + 3A_2^2 \overline{A}_2 e^{i\omega_2 T_0}) \\ &- \alpha_4 (A_1 A_2^2 e^{i(\omega_1 + 2\omega_2)T_0} \\ &+ 2A_1 A_2 \overline{A}_2 e^{i\omega_1 T_0} \\ &+ \overline{A}_1 A_2^2 e^{i(-\omega_1 + 2\omega_2)T_0}) \end{aligned} \tag{11}$$

$$
\begin{aligned}
&- \alpha_5(A_1^3 e^{3i\omega_1 T_0} \\
&+ 3A_1^2 \bar{A}_1 e^{i\omega_1 T_0}) \\
&- \alpha_6(A_1 A_3^2 e^{i(\omega_1 + 2\omega_3)T_0} \\
&+ 2A_1 A_3 \bar{A}_3 e^{i\omega_1 T_0} \\
&+ \bar{A}_1 A_3^2 e^{i(-\omega_1 + 2\omega_3)T_0}) \\
&+ \hat{f}_1(t) + cc
\end{aligned}
$$

$$
\begin{aligned}
&D_0^2 x_{21} + \omega_2^2 x_{21} = -2A_2' i\omega_2 e^{i\omega_2 T_0} \\
&- 2\mu_2 A_2 i\omega_2^2 e^{i\omega_2 T_0} \\
&- \alpha_7(A_1 A_3 e^{i(\omega_1 + \omega_2)T_0} + \bar{A}_1 A_3 e^{i(\omega_3 - \omega_1)T_0}) \\
&- \alpha_8(A_2^3 e^{3i\omega_2 T_0} + 3A_2^2 \bar{A}_2 e^{i\omega_2 T_0}) \\
&- \alpha_9(A_1 A_2^2 e^{i(\omega_1 + 2\omega_2)T_0} + 2A_1 A_2 \bar{A}_2 e^{i\omega_1 T_0} \\
&+ \bar{A}_1 A_2^2 e^{i(-\omega_1 + 2\omega_2)T_0}) \\
&- \alpha_{10}(A_1^2 A_2 e^{i(2\omega_1 + \omega_2)T_0} + 2A_1 \bar{A}_1 A_2 e^{i\omega_2 T_0} \\
&+ A_1^2 \bar{A}_2 e^{i(2\omega_1 - \omega_2)T_0}) - \alpha_{11}(A_2 A_3^2 e^{i(\omega_2 + 2\omega_1)T_0} \\
&+ 2A_2 A_3 \bar{A}_3 e^{i\omega_2 T_0} \\
&+ \bar{A}_2 A_3^2 e^{i(-\omega_2 + 2\omega_1)T_0}) + \hat{f}_2(t) + cc
\end{aligned}
\tag{12}
$$

$$
\begin{aligned}
&D_0^2 x_{31} + \omega_3^2 x_{31} = -2A_3' i\omega_3 e^{i\omega_3 T_0} \\
&- 2\mu_3 A_3 i\omega_3^2 e^{i\omega_3 T_0} - \alpha_{12}(A_1^2 e^{2i\omega_1 T_0} \\
&+ A_1 \bar{A}_1) - \alpha_{13}(A_1 A_2 e^{i(\omega_1 + \omega_2)T_0} \\
&+ A_1 \bar{A}_2 e^{i(\omega_1 - \omega_2)T_0}) - \alpha_{14}(A_2^2 A_3 e^{i(2\omega_2 + \omega_3)T_0} \\
&+ 2A_2 \bar{A}_2 A_3 e^{i\omega_3 T_0} + A_2^2 \bar{A}_3 e^{i(2\omega_2 - \omega_3)T_0}) \\
&- \alpha_{15}(A_1^2 A_3 e^{i(2\omega_1 + \omega_3)T_0} + 2A_1 \bar{A}_1 A_3 e^{i\omega_3 T_0} \\
&+ A_1^2 \bar{A}_3 e^{i(2\omega_1 - \omega_3)T_0}) - \alpha_{16}(A_3^3 e^{3i\omega_3 T_0} \\
&+ 3A_3^2 \bar{A}_3 e^{i\omega_3 T_0}) + \hat{f}_3(t) + cc
\end{aligned}
\tag{13}
$$

where $\bar{A}_j$ denotes the complex conjugate of A_j. Since we require the solutions to be uniformly valid in time*, any term on the right hand side of Eqs (11), (12), and (13) that would cause x_{j1} to grow unbounded, must be neglected. Such terms are called secular producing and will be of the form $(\ )e^{i\omega_j T_0}$ for $j = 1$, 2, and 3 in Eqs (11), (12), (13) respectively. In this way the expressions for the A_j are determined.

3.2 Possible Secular Producing Terms

Clearly there are a vast number of secular producing terms depending on relationships between ω_1, ω_2, ω_3 and the frequencies of the external forces. In the next section, these many possibilities are limited to those which have physical significance for an in-line four cylinder engine at hot idle.

* For the notation used here, the approximation for $X_i(t;\epsilon)$ of Eq. (5) should be such that small terms remain small for all time. That is, if x_{i0} is the principal term in the approximation and x_{i1} is the correction to it, we want $|\epsilon x_{i1}| \ll |x_{i0}|$ for all time. As presented in Kahn [8], when this is accomplished, the resulting approximation is said to be uniformly valid in time.

4. System Response

In this section, the frequency response of the system is presented. We first discuss the source of the forcing terms, their likely form, and then identify the resulting secular producing terms in Eqs (11), (12), and (13). An example problem that considers forcing in the vertical and rotational directions is then presented.

4.1 Source of Forcing Terms

When one discusses the internal forces generated in an engine, it is typical to represent the horizontal, torsional, and vertical components of force in the form

$$
\begin{aligned}
f_j(t) &= f_{j1}\cos(\Omega t) + f_{j2}\cos(2\Omega t) \\
&+ \ldots + f_{jn}\cos(n\Omega t) \text{ for } j = 1, 2, 3
\end{aligned}
$$

respectively, and where Ω is the engine rotational speed. The integer n describes the order of the unbalance. The case of $n = 1$ is called the first order or primary unbalance force. The case of $n = 2$ is similarly called the second order or secondary unbalance. Ideally, a perfectly balanced engine would have all f_{jn} equal to zero at all engine speeds. For an in-line four cylinder engine, all the first order forces and moments are theoretically balanced while certain second order forces and moments are unbalanced, as presented in Den Hartog [9]. However, it has been found that in actual engines the first order moments in the X_2 direction (torsional), do not completely balance, Whitekus [10]. For the X_3 direction (vertical), unbalance appears at the second order. Table 1 depicts these results in tabular form.

Typically, the six rigid body linear natural frequencies of an automotive engine lie between 5 Hz and 25 Hz. It is not unreasonable to expect that there could be nearly simple integer relationships between several of the linear natural frequencies. Several papers which list the six linear natural frequencies for actual engines indicate that such relationships do occur in actual engines. See Johnson and Subhedar [11], Geck and Patton [12] and Spiekerman, *et al.* [13] Guided by these works and the information in Table 1, the relationships between the linear natural frequencies chosen for this study are the following:

Table 1. Summary of forcing conditions.

	1st Order oscillation at engine speed	2nd Order oscillation at 2× engine speed
Unbalanced horizontal force (X_1 direction)	$f_{11} = 0$	$f_{12} = 0$
Unbalanced vertical force (X_3 direction)	$f_{31} = 0$	$f_{32} \neq 0$
Unbalanced moment (X_2 direction)	$f_{21} \neq 0$	$f_{22} = 0$

$$\omega_1 \approx \omega_2, 2\omega_1 \approx \omega_3 \text{ and } \Omega \approx \omega_2 \tag{14}$$

with

$$\hat{f}_1(t) = 0, \tag{15a}$$

$$\hat{f}_2(t) = \hat{f}_{21}\cos(\Omega t) \tag{15b}$$

$$\hat{f}_3(t) = \hat{f}_{32}\cos(2\Omega t) \tag{16}$$

The second order component of $\hat{f}_2$ is neglected as it is typically much smaller than the first order component.

4.2 System Parameter Values

Prior to presenting the frequency response plots, discussion of the parameter values to be used in the numerical analysis is needed. The physical dimensions of the rigid body are representative of the dimensions of an engine viewed along the crankshaft axis. The system parameters as shown in Figs 1 and 2 are:

Mass m:	219.4 kg
Inertia I_G:	14.155 kg m^2
Height $2B$:	0.842 m
Width $2A$:	0.254 m
k_1:	1,732,312.8 N/m
k_2:	433,078.2 N/m
k_3:	433,078.2 N/m
k_4:	1,732,312.8 N/m

These parameter values are used to obtain the numerical coefficients of the terms of the Taylor series approximation of the potential energy about the static equilibrium point. These coefficients are then divided appropriately by either m or I_G producing the α's given in Eqs (1), (2), and (3). The resulting numerical values of the α's are:

α_1 =	−4915.45	α_9 =	−58,055.75
α_2 =	154,817.68	α_{10} =	−474,311.20
α_3 =	−1248.52	α_{11} =	180,387.67
α_4 =	−30,601.07	α_{12} =	77,408.84
α_5 =	758,908.77	α_{13} =	−4915.45
α_6 =	−1,897,270.97	α_{14} =	11,638.05
α_7 =	−76,188.63	α_{15} =	−1,897,270.97
α_8 =	−144.52	α_{16} =	189,727.10

The values of the damping coefficients c_1, c_2, and c_3 were chosen such that the viscous damping ratios of the linearized system equal 0.01 for all modes, i.e. $\epsilon\mu_j$ in Eqs (1), (2), and (3) are such that $\epsilon\mu_j = 0.01$.

The forcing terms were chosen to be of the same order of magnitude as the force found in production engines. For a nominal rotational engine speed of 600 rpm, the values used are:

$$\epsilon\hat{f}_2 = \epsilon\hat{f}_{21}\cos(\Omega t) = 30\cos(20\pi t)\text{ N m}$$

$$\epsilon\hat{f}_3 = \epsilon\hat{f}_{32}\cos(2\Omega t) = 500\cos(40\pi t)\text{ N}$$

The parameter ϵ introduced in Eqs (1), (2), and (3) must be specified to enable the numerical evaluation of the results of the multiple scales analysis of the rigid body system. The value of ϵ used here is 0.01. The ramifications of the choice of the value of ϵ are discussed in Kahn [8].

4.3 Example: Combined Torsional and Vertical Unbalanced Forces

The considerations of the previous sections regarding the physical system are used in this section to determine the secular producing terms in Eqs (11), (12), and (13). Using the relationships given in Eqs (15) and (16), forcing in both the X_2 and X_3 coordinate directions is present. Hence we have respectively, $\hat{f}_2(t) = \hat{f}_{21}\cos(\Omega t)$, and $\hat{f}_3(t) = \hat{f}_{32}\cos(2\Omega t)$.

The relationships between the natural frequencies, given in Eq. (14), and the forcing frequency are now used to determine the secular conditions. Consistent with the method of multiple scales, detuning parameters are introduced. These detuning parameters are represented by σ_m's such that:

$$\Omega = \omega_2 + \epsilon\sigma_1 \tag{17}$$

and

$$\omega_2 = \omega_1 - \epsilon\sigma_2,\ \omega_3 = 2\omega_1 - \epsilon\sigma_3 \tag{18}$$

Using these relationships, the secular terms in Eqs (11), (12), and (13) are eliminated by letting:

$$\begin{aligned}&-2A_1'i\omega_1 - 2\mu_1A_1i\omega_1^2 - \alpha_1\bar{A}_2A_3e^{i(\sigma_2-\sigma_3)T_1}\\&-\alpha_2\bar{A}_1A_3e^{-i\omega_3T_1} - 3\alpha_3A_2^2\bar{A}_2e^{-i\sigma_2T_1}\\&-\alpha_4(2A_1A_2\bar{A}_2 + \bar{A}_1A_2^2e^{-2i\sigma_2T_1}) - 3\alpha_5A_1^2\bar{A}_1\\&-2\alpha_6A_1A_3\bar{A}_3 = 0\end{aligned} \tag{19}$$

$$\begin{aligned}&-2A_2'i\omega_2 - 2\mu_2A_2i\omega_2^2 - \alpha_7\bar{A}_1A_3e^{i(\sigma_2-\sigma_3)T_1}\\&-3\alpha_8A_2^2\bar{A}_2 - \alpha_9(2A_1A_2\bar{A}_2e^{i\sigma_2T_0}\\&+\bar{A}_1A_2^2e^{-i\sigma_2T_1}) - \alpha_{10}(2A_1\bar{A}_1A_2 + A_1^2\bar{A}_2e^{2i\sigma_2T_1})\\&-2\alpha_{11}A_2A_3\bar{A}_3 + \frac{\hat{f}_{21}}{2}e^{i\sigma_1T_1} = 0\end{aligned} \tag{20}$$

$$\begin{aligned}&-2A_3'i\omega_3 - 2\mu_3A_3i\omega_3^2 - \alpha_{12}A_1^2e^{i\sigma_3T_1}\\&-\alpha_{13}A_1A_2e^{i(\sigma_3-\sigma_2)T_1} - 2\alpha_{14}A_2\bar{A}_2A_3\\&-2\alpha_{15}A_1\bar{A}_1A_3 - 3\alpha_{16}A_3^2\bar{A}_3\\&+\frac{\hat{f}_{32}}{2}e^{i(2\sigma_1-2\sigma_2+\sigma_3)T_1} = 0\end{aligned} \tag{21}$$

These equations are then put in autonomous form and the real and imaginary parts are separated from each other giving the following six equations governing the amplitude modulations in time T_1:

$$\begin{aligned}u_1' &= u_2(\sigma_1-\sigma_2) - \mu_1\omega_1u_1 - \frac{\alpha_1}{4\omega_1}(u_3u_6 - u_4u_5)\\&-\frac{\alpha_2}{4\omega_1}(u_1u_6 - u_2u_5) - \frac{3\alpha_3}{8\omega_1}(u_3^2u_4 + u_4^3)\\&-\frac{\alpha_4}{8\omega_1}(u_2u_3^2 + 3u_2u_4^2 + 2u_1u_3u_4)\\&-\frac{3\alpha_5}{8\omega_1}(u_1^2u_2 + u_2^3) - \frac{\alpha_6}{4\omega_1}(u_2u_5^2 + u_2u_6^2)\end{aligned} \tag{22}$$

$$u_2' = -u_1(\sigma_1 - \sigma_2) - \mu_1\omega_1 u_2 + \frac{\alpha_1}{4\omega_1}(u_3u_5 + u_4u_6) + \frac{\alpha_2}{4\omega_1}(u_1u_5 + u_2u_6) + \frac{3\alpha_3}{8\omega_1}(u_3^3 + u_3u_4^2) + \frac{\alpha_4}{8\omega_1}(3u_1u_3^2 + u_1u_4^2 + 2u_2u_3u_4) + \frac{3\alpha_5}{8\omega_1}(u_1^3 + u_1u_2^2) + \frac{\alpha_6}{4\omega_1}(u_1u_5^2 + u_1u_6^2) \quad (23)$$

$$u_3' = u_4\sigma_1 - \mu_2\omega_2 u_3 - \frac{\alpha_7}{4\omega_2}(u_1u_6 - u_2u_5) - \frac{3\alpha_8}{8\omega_2}(u_3^2u_4 + u_4^3) - \frac{\alpha_9}{8\omega_2}(u_2u_3^2 + 3u_2u_4^2 + 2u_1u_3u_4) - \frac{\alpha_{10}}{8\omega_2}(u_1^2u_4 + 3u_2^2u_4 + 2u_1u_2u_3) - \frac{\alpha_{11}}{4\omega_2}(u_4u_5^2 + u_4u_6^2) \quad (24)$$

$$u_4' = -u_3\sigma_1 - \mu_2\omega_2 u_4 + \frac{\alpha_7}{4\omega_2}(u_1u_5 + u_2u_6) + \frac{3\alpha_8}{8\omega_2}(u_3^3 + u_3u_4^2) + \frac{\alpha_9}{8\omega_2}(3u_1u_3^2 + u_1u_4^2 + 2u_2u_3u_4) + \frac{\alpha_{10}}{8\omega_2}(3u_1^2u_3 + u_2^2u_3 + 2u_1u_2u_4) - \frac{\alpha_{11}}{4\omega_2}(u_3u_5^2 + u_3u_6^2) - \frac{\hat{f}_{21}}{2\omega_2} \quad (25)$$

$$u_5' = u_6(2\sigma_1 - 2\sigma_2 + \sigma_3) - \mu_3\omega_3 u_5 - \frac{\alpha_{12}}{2\omega_3}u_1u_2 - \frac{\alpha_{13}}{4\omega_3}(u_1u_4 + u_2u_3) - \frac{\alpha_{14}}{4\omega_3}(u_3^2u_6 + u_4^2u_6) - \frac{\alpha_{15}}{4\omega_3}(u_1^2u_6 + u_2^2u_6) - \frac{3\alpha_{16}}{8\omega_3}(u_5^2u_6 + u_6^3) \quad (26)$$

$$u_6' = -u_5(2\sigma_1 - 2\sigma_2 + \sigma_3) - \mu_3\omega_3 u_6 + \frac{\alpha_{12}}{4\omega_3}(u_1^2 - u_2^2) + \frac{\alpha_{13}}{4\omega_3}(u_1u_3 - u_2u_4) + \frac{\alpha_{14}}{4\omega_3}(u_3^2u_5 + u_4^2u_5) + \frac{\alpha_{15}}{4\omega_3}(u_1^2u_5 + u_2^2u_5) + \frac{3\alpha_{16}}{8\omega_3}(u_5^3 + u_5u_6^2) - \frac{\hat{f}_{32}}{2\omega_3} \quad (27)$$

These equations are frequently referred to as reduced equations or as slowly varying equations. The relationship between the u_i of the reduced equations and the X_j of the equations of motion is:

$$X_1(t) \approx x_{10}(t) = \sqrt{u_1^2 + u_2^2}\cos(\Omega t + \gamma_1) \quad (28)$$

where $\gamma_1 = \tan^{-1}\left[\frac{u_2}{u_1}\right]$

$$X_2(t) \approx x_{20}(t) = \sqrt{u_3^2 + u_4^2}\cos(\Omega t + \gamma_2) \quad (29)$$

where $\gamma_2 = \tan^{-1}\left[\frac{u_4}{u_3}\right]$

$$X_3(t) \approx x_{30}(t) = \sqrt{u_5^2 + u_6^2}\cos(2\Omega t + \gamma_3) \quad (30)$$

where $\gamma_3 = \tan^{-1}\left[\frac{u_6}{u_5}\right]$

The utility of Eqs (22)–(27) extends beyond the fact that they govern the amplitude modulations of the X_j in time T_1. Setting the time derivatives of the equations, i.e. the left hand sides, equal to zero produces six nonlinear algebraic equations. The solutions of these equations are the steady state amplitudes of the X_j. These algebraic equations can be solved for ranges of σ_m to produce frequency response plots.

4.3.1 Stability Issues

Prior to using these equations to produce response plots, the stability of the solutions is discussed. Consider Eqs (22)–(27) written in vector notation, as follows:

$$\boldsymbol{x}' = \boldsymbol{f}(\boldsymbol{x}) \quad (31)$$

Into this equation can be substituted a vector $\boldsymbol{x}_s$ with:

$$\boldsymbol{x}_s = \boldsymbol{x}_{ss} + \boldsymbol{x}_p \quad (32)$$

where $\boldsymbol{x}_{ss}$ is the actual steady state solution and $\boldsymbol{x}_p$ is a small perturbation of the actual steady state solution. The notion of this exercise is that if $\boldsymbol{x}_p \to 0$ as $t \to \infty$, then the solution $\boldsymbol{x}_{ss}$ is considered stable.

Next, consider a Taylor series expansion in one variable of $\boldsymbol{f}(\boldsymbol{x}_{ss} + \boldsymbol{x}_p)$ about $\boldsymbol{x}_p$:

$$\boldsymbol{f}(\boldsymbol{x}_{ss} + \mathbf{x}_p) = \boldsymbol{f}(\boldsymbol{x}_{ss}) + \left[\frac{\partial \boldsymbol{f}(\boldsymbol{x}_{ss})}{\partial \boldsymbol{x}}\right]\boldsymbol{x}_p + O(\boldsymbol{x}_p^2) \quad (33)$$

Note that $\boldsymbol{f}(\boldsymbol{x}_{ss}) = 0$ by definition and also that

$$(\boldsymbol{x}_{ss} + \boldsymbol{x}_p)' = \boldsymbol{x}_p' = \mathbf{f}(\boldsymbol{x}_{ss} + \mathbf{x}_p) \quad (34)$$

Hence Eq. (33) can be written as follows:

$$\boldsymbol{x}' = \left[\frac{\partial \boldsymbol{f}(\boldsymbol{x}_{ss})}{\partial \boldsymbol{x}}\right]\boldsymbol{x}_p \quad (35)$$

Equation (35) is a set of autonomous linear ordinary differential equations with constant coefficients. It can be shown, see Derrick and Grossman [14], that the eigenvalues of the coefficient matrix given in Eq. (35) denote the stability of the system for $\boldsymbol{x} = \boldsymbol{x}_{ss}$. This coefficient matrix is referred to as the Jacobian matrix. This method of examining the eigenvalues of the Jacobian matrix is used to establish the stality of the solutions of Eqs (22)–(27).

4.3.2 Amplitude Frequency Plots

The six algebraic equations governing the steady state amplitudes for the system are given by Eqs (22)–(27) with the terms containing the time derivatives set

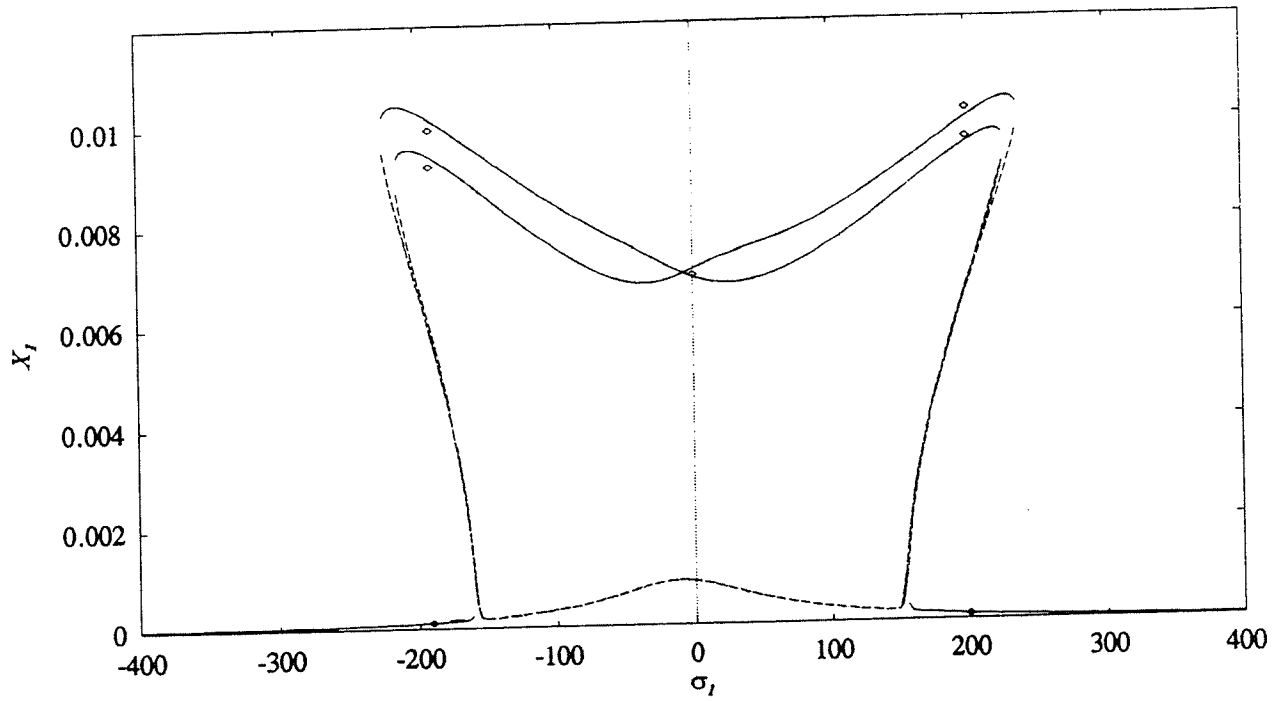

Fig. 3. Frequency response for X_1 (horizontal response). Solid line – stable solution; dotted line – unstable solution.

equal to zero. A representative set of response plots are shown in Figs 3, 4, and 5. For this example it is assumed that there is perfect tuning between the natural frequencies, i.e., $\omega_1 = \omega_2$ and $2\omega_1 = \omega_3$ and hence the detuning parameters σ_2 and σ_3, as defined in Eq. (18), are both zero. The remaining detuning parameter, σ_1, measures the nearness of the forcing frequency, Ω, to ω_2 (see Eq. (17)). It should be recalled that in this example, forcing is applied only in the X_2 and X_3 directions (rotational and vertical, respectively). The associated forcing frequencies are Ω and 2Ω, respectively. Hence, from a linear system

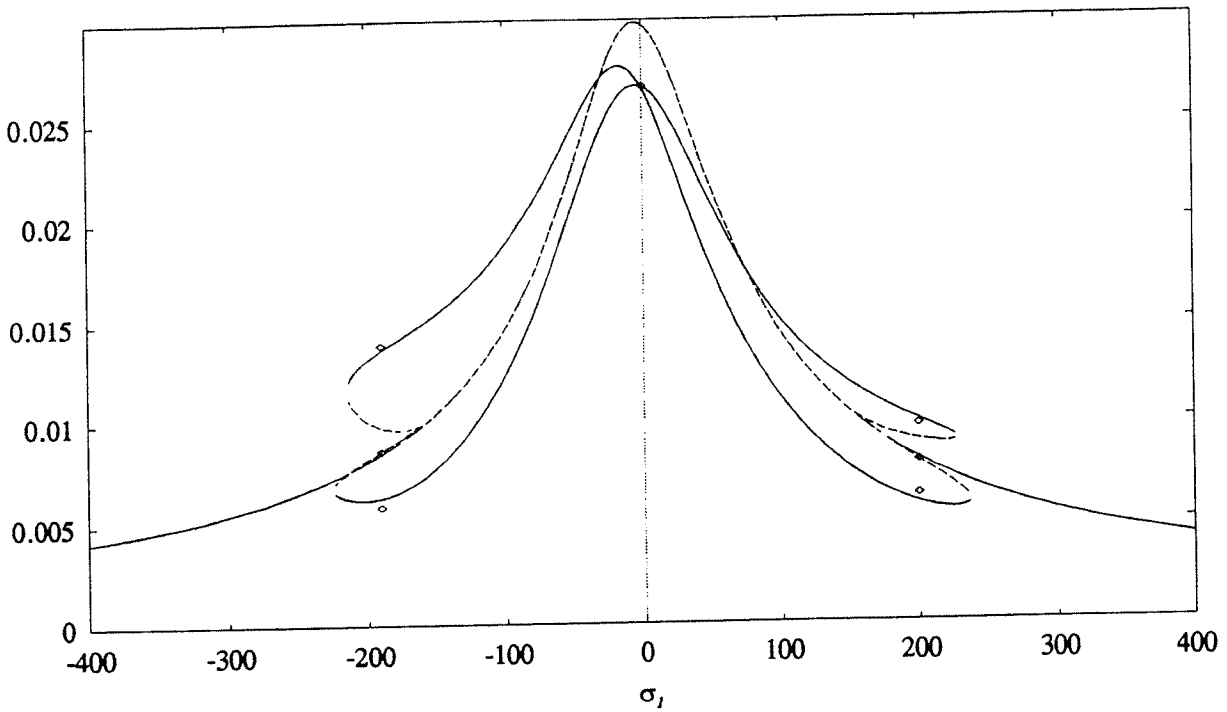

Fig. 4. Frequency response for X_2 (rotational response). Solid line – stable solution; dotted line – unstable solution.

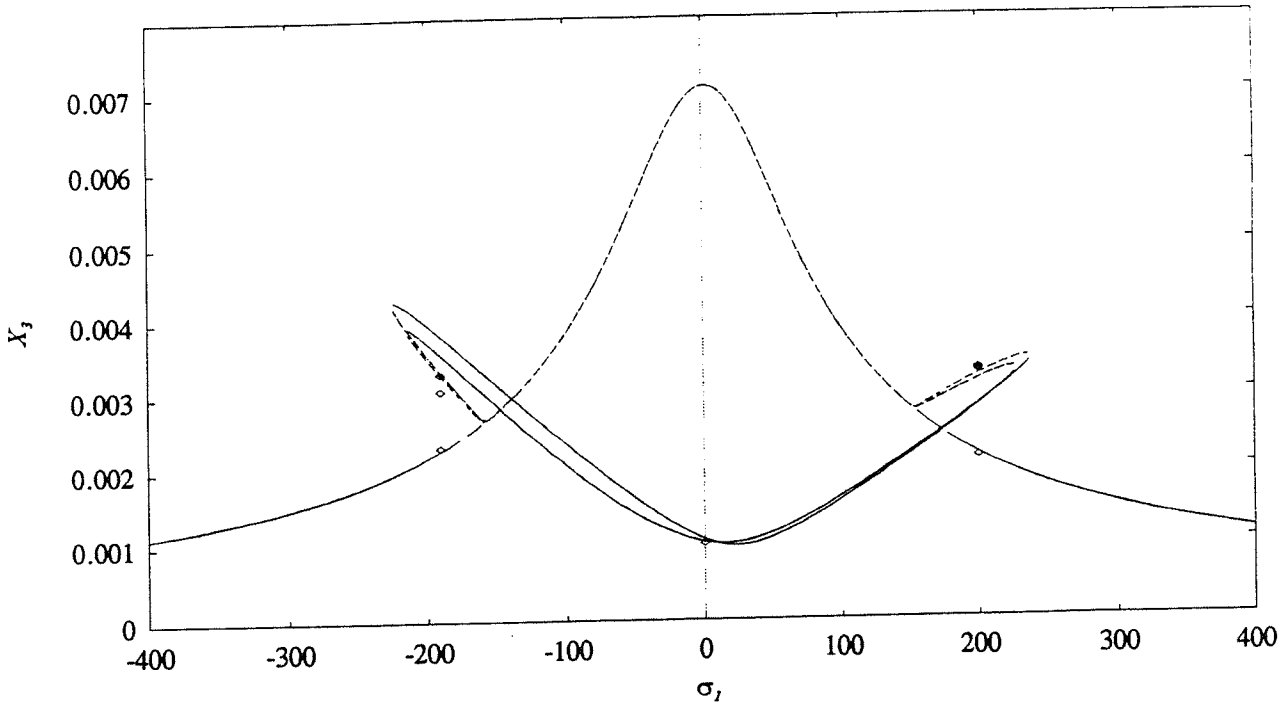

Fig. 5. Frequency response for X_3 (vertical response). Solid line – stable solution; dotted line – unstable solution.

standpoint, one would expect to see resonant responses of the X_2 and X_3 coordinates only and for the X_1 coordinate to remain small.

Figure 3 shows that this is not the case. Here it is seen that over the range $-200 \leqslant \sigma_1 \leqslant 230$, the response of this coordinate is both resonant and multi-valued. In the regions $-200 \leqslant \sigma_1 \leqslant -160$ and $150 \leqslant \sigma_1 \leqslant 240$ the response is triple valued. The responses of coordinates X_2 and X_3, shown in Figs 4 and 5 respectively, also exhibit similar features. Due to the geometry of the system and the resulting nonlinearities, there is a transfer of energy between the modes. Of particular benefit to the automotive industry is the reduction of the vertical motion (X_3) over a wide range of the forcing frequency. Of course there is an associated increase in the horizontal (unforced X_1 coordinate) but typically this is a much more acceptable motion to have in automotive applications.

For this case, verification of the response magnitudes for each of the three system coordinates was made. The verification is made through comparison with the response amplitudes predicted through numerical integration of Eqs (1), (2), and (3) to those predicted by the steady state values obtained from the reduced equations. The comparisons were made only for selected values of σ_1: $\sigma_1 = \pm 180$, $\sigma_1 = 200$, and $\sigma_1 = 0$. These amplitudes are indicated in Figs 3, 4, and 5 by the diamond mark. This comparison shows that the approximate solution technique is accurate, at least for the limited cases tested.

It is seen that a large reduction in amplitude is realized in the X_3 coordinate response for the range $-120 \leqslant \sigma_1 \leqslant 150$. It is in this range that the nonlinear system produces a small response compared to the linear response. This difference in amplitudes can be utilized to enhance the isolation response of the system. It is this fact that is investigated in Section 5.

5. Isolation Characteristics

With the frequency response of the system established, its isolation characteristics can be investigated. An overview of vibration isolation metrics is presented in the first section. In the second section, the isolation performance of the rigid body system is analysed.

5.1 Discussion of Vibration Isolation Metrics

Various metrics have been applied to the evaluation of vibration isolation systems. The three measures prevalent in literature are transmissibility, isolation effectiveness, and power transmission. It is the purpose here to briefly consider each of these measures and then to extend the concept of the force transmitted to the base.

The idea of transmissibility for a damped, linear single degree of freedom system under harmonic excitation is well established. It is commonly defined as either the ratio of the force transmitted to the base to the applied force, see Sykes, [15], and Ungar and Dietrich, [16], or alternatively for a single mass undergoing base excitation, it is defined as the ratio

of the base motion to the displacement of the system mass.

Another measure of isolator performance is effectiveness, see Sykes, [15] and Ungar and Dietrich, [16]. This quantity is also referred to as isolator effectiveness, isolation effectiveness, and insertion loss, see Rubin and Biehl, [17]. Effectiveness is a nondimensional measure of the reduction of the vibration of a system. It is defined as the ratio of the structural vibration of the system with no isolator (the source and receiver are rigidly connected) to the structural vibration of the isolated system. If this ratio is greater than unity, the isolator reduces the amplitude of the receiver response. If this ratio is less than unity, the isolator increases the amplitude of the receiver response. Recently, the notion of effectiveness has been expended by Swanson *et al.*, [18] to systems that include multiple parallel isolators connecting one mass to a foundation.

Another metric for vibration isolation systems is that of power transmission, or power flow as defined in Pinnington, [19], and Qu and Qian, [20]. The expression for the time averaged power transmission due to a harmonic input for multiple input, multiple isolator system is given by Pinnington, [19]:

$$\omega P = \frac{1}{2}\,\mathrm{Im}\{[F^{*}]^{T}[A][F]\} \tag{36}$$

where $[F]$ is the vector of applied forces, $[A]$ is the accelerance matrix, and ω is the frequency of the applied force. The superscript T denotes the transpose and the superscript * denotes the complex conjugate. Further qualification of this expression is presented for broadband application where spectral densities are used. Correlation between the analytical method and an experimental system is presented in the cited work.

All of these metrics are derived under the assumption that the system under investigation responds linearly. No provision is made in any of the metrics for nonlinear system response. Moreover, the effectiveness and transmissibility metrics assume that the chosen system response variable (force, velocity, displacement, etc.) is rectilinear in nature. Application of these metrics to general rigid body vibration isolation problems would be inappropriate, as the system response is typically no rectilinear. Additionally, for the transmissibility and effectiveness metrics as applied, the assumption is made that the disturbance and the response are collinear. Thus, a single isolator does not isolate in more than one direction. As such, the vectorial aspects of the response are neglected and the actual effectiveness of the isolation system cannot be captured using these metrics. Furthermore, for nonlinear systems, small changes in the harmonic force acting on a rigid body on resilient supports can lead to pronounced changes in the system response. This situation can affect the direction of the reaction force at the point of connection between the isolator and the foundation. Therefore, the general response of the system must be investigated in order to completely capture the system response and isolation performance.

5.2 Measure of Isolation Efficiency

Assessment of the isolation performance of the system is now developed. The metric chosen for application to this system is the forces transmitted to the base. Two modifications are required to adapt this metric to account for the nonlinear response of the system. The first modification develops the capability to account for the presence of more than one frequency in the system response. The response for this system is comprised of two frequencies and is periodic. Therefore, the root-mean-square (rms) of the response is used to account for multiple frequencies.

The second modification to this metric is made to permit system response in all three degrees of freedom to be accounted. This is done by using the forces transmitted to the base developed in each of the springs in the system model. These forces are due to the response contributed by each of the three degrees of freedom and therefore will account for the total motion of the rigid body.

Using these two modifications, the force used in the metric can be computed. First, the vertical and horizontal components of the forces for each of the springs (F_{1x} and F_{1y} for k_1, F_{2x} and F_{2y} for k_2, F_{3x} and F_{3y} for k_3, F_{4x} and F_{4y} for k_4) represented here as x and y respectively, are computed. The total force from each pair of springs on the foundation is due to the deflection of the pairs of springs l_1 and k_2, and k_3 and k_4, given by F_{12} and F_{34} respectively. These forces are given by:

$$F_{12}(t) = \sqrt{(F_{1x} + F_{2x})^2 + (F_{1y} + F_{2y})^2} \tag{37}$$

$$F_{34}(t) = \sqrt{(F_{3x} + F_{4x})^2 + (F_{3y} + F_{4y})^2} \tag{38}$$

These forces are time dependent. Therefore, the rms value of each of these forces is computed and then summed:

$$F = (F_{12})_{\mathrm{rms}} + (F_{34})_{\mathrm{rms}} \tag{39}$$

It is this force, F, that is used to assess the isolation performance of the rigid body system.

Figure 6 shows a plot of the magnitude of the force given in Eq. (39) as a function of the detuning parameter σ_1 for the system under investigation. This figure also contains the frequency response of the linear system. Here, the linear system response was computed using Eq. (39) after setting the coefficients of the nonlinear terms to zero.

From Fig. 6, it can be seen that in the region between $\sigma_1 \approx \pm 125$, the force transmitted to the foundation for the nonlinear system, which can be either of two stable solutions, is reduced in comparison with the forces transmitted by the equivalent linear system. In particular, the large peak in the response for the linear system is eliminated. This performance

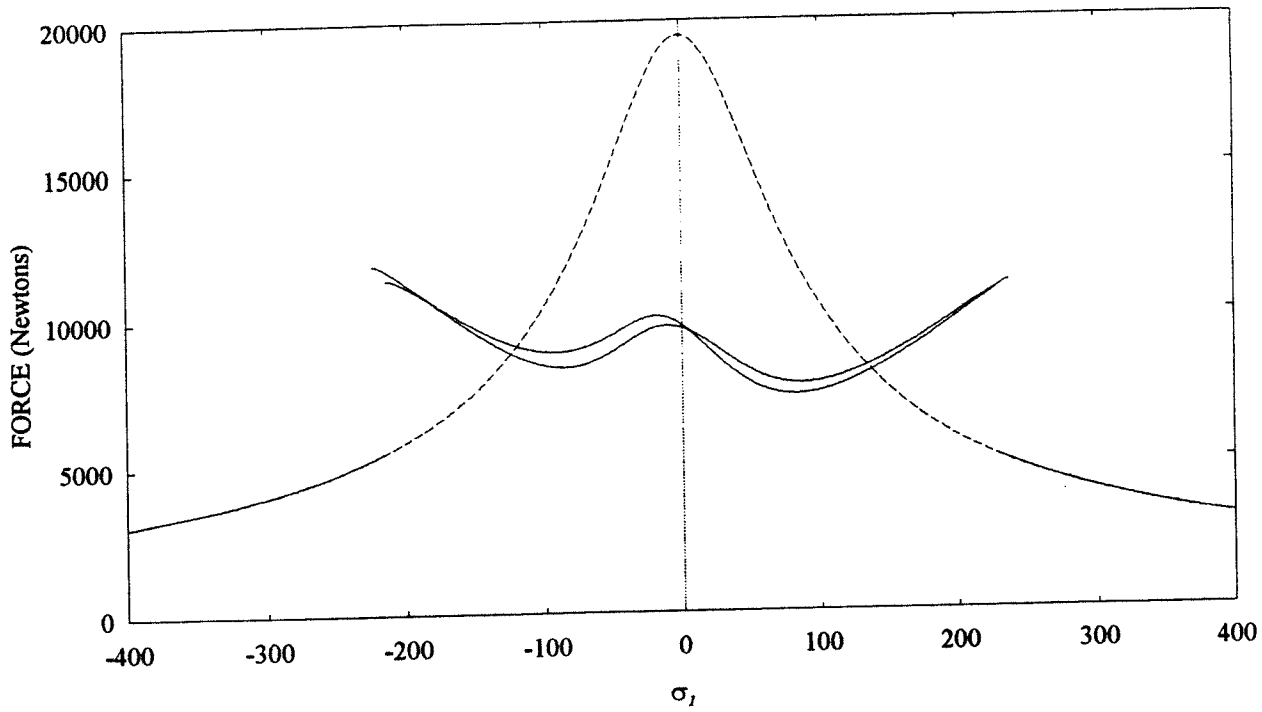

Fig. 6. Response plot of the force transmitted to the base. Solid line – stable solution; dotted line – unstable solution.

advantage is lost in the regions $228 > \sigma_1 > 125$ and $-125 > \sigma_1 > -228$, where the transmitted forces of the nonlinear system are greater than the forces of the corresponding linear system. For $\sigma_1 > 228$ and $\sigma_1 < -228$, the linear and nonlinear solutions are identical and no advantage is realized from the nonlinear system. In these regions, the transmitted forces are much lower than those associated with the linear resonance condition and are typically of less concern.

This analysis illustrates the need for proper system modelling. Modelling this system using linear theory leads to the incorrect system response which predicts that a large peak in the transmitted forces will result near $\sigma_1 = 0$.

6. Concluding Remarks

The equations for the planar motion of a rigid body have been presented, the geometry and typical system parameter values being based on a generic in-line, four cylinder automotive engine. At idle speeds, the dominant forcing terms arise from unbalanced internal forces, as opposed to base motions. Although these forces generate relatively small displacements, it has clearly been shown that geometric nonlinearities must be accounted for when modelling the system.

Having analysed the response of the various modes, it was then shown that the traditional measures of isolation performance, i.e., effectiveness, transmissibility, and transmitted power, have shortcomings when applied to nonlinear systems. Specifically, these metrics do not account for the multi-frequency response of nonlinear systems. In addition, effectiveness and transmissibility do not account for system response in coordinate directions different from the direction of the input force. However, these two aspects of nonlinear system response were incorporated into a modified metric for assessing the forces transmitted to the foundation. This metric was then applied to the rigid body problem studied herein.

References

1. Nayfeh A H, Mook D T. Nonlinear oscillations. Wiley-Interscience, John Wiley & Sons, New York, 1979
2. Henry R F, Tobias S A. Instability and steady-state coupled motions in vibration isolating suspensions. Journal Mechanical Engineering Science, 1959; 1(1): 19–29
3. Henry R F, Tobias S A. Modes at rest and their stability in coupled non-linear systems. Journal Mechanical Engineering Science, 1961; 3(2): 163–173
4. Grootenhuis P, Ewins D J. Vibration of a spring supported body. Journal Mechanical Engineering Science 1965; 7(2): 185–192
5. Efstathiades G J, Williams C J H. Vibration isolation using nonlinear springs. J. Mech. Sci., 1967; 9: 27–44
6. Brach R Matthew. Harmonic response and vibration isolation of rigid bodies. Ph.D. Thesis, Michigan State University, East Lansing, MI, 1995
7. Wolfram S. Mathematica: A system for doing mathematics by computer. Addison-Wesley, Redwood City, CA, 1991
8. Kahn P B. Mathematical methods for scientists and engineers. Wiley-Interscience, John Wiley & Sons, New York, 1991

9. Den Hartog J P. Mechanical vibrations (4th ed.), McGraw-Hill, New York, 1956
10. Whitekus J D. Personal communication at the Ford Motor Company, August 3, 1994
11. Johnson Stephen R, Subhedar Jay W. Computer optimization of engine mount systems. SAE Paper 790974, SAE, Warrendale, PA, 1979
12. Geck Paul E, Patton R D. Front wheel engine mount optimization. SAE Paper 840736, Warrendale, PA, 1984
13. Spiekerman C E, Radcliffe C J, Goodman E D. Optimal design and simulation of vibration isolation systems. Journal of Mechanisms, Transmission and Automation in Design, 1985; 107: 271–276
14. Derrick W R, Grossman S I. Introduction to differential equations with boundary value problems. (3rd ed.) West Publishing Co., St. Paul, MN, 1987
15. Sykes A O. The evaluation of mounts isolating nonrigid machines from nonrigid foundations. Shock and Vibration Instrumentation, New York: ASME, 1956
16. Ungar E E, Dietrich C W. High-frequency vibration isolation, Journal of Sound and Vibration 1966; 4(2): 224–241
17. Rubin S, Biehl F A. Mechanical impedance approach to engine vibration transmission into an aircraft fuselage, SAE Paper 670873, SAE, Warrendale, PA, 1967
18. Swanson D A, Miller L R, Norris M A. Multidimensional mount effectiveness for vibration isolation. Journal of Aircraft, 1994; 31(1): 188–196
19. Pinnington R J. Vibrational power transmission to a seating of a vibration isolated motor. Journal of Sound and Vibration 1987; 118(3): 515–530
20. Qu J, Qian B. On the vibrational power flow from engine to elastic structure through single and double resilient mounting systems. SAE Paper 911057, SAE, Warrendale, PA, 1991

Nomenclature

A	half width of the rigid body (m)
B	half height of the rigid body (m)
c_j	coefficient of viscous damping
D_j	time derivative with respect to time T_i
F	force transmitted to the foundation
f_i	force associated with coordinate direction X_i
$\bar{f}_i$	rescaled form of f_i
F_T	transmitted force (N)
I_G	mass moment of inertia (m^2 kg)
k_i	spring constant (N/m)
m	mass (kg)
T_n	time scale
X_1, X_2, X_3	horizontal, rotational, and vertical coordinate variables respectively
α_m	coefficients of the nonlinear terms
γ_j	phase parameter
ϵ	small dimensionless parameter used in multiple scales analysis
μ_j	dimensioness damping coefficient
σ_j	detuning parameter
ω_1, ω_2, ω_3	natural frequency (rad/s)
Ω	forcing frequency (rad/s)